Journal of Alloys and Compounds 495 (2010) 578–582

Contents lists available at ScienceDirect

Journal of Alloys and Compounds

journal homepage: www.elsevier.com/locate/jallcom

Nanostructured aluminium oxide powders obtained by aspartic acid–nitrate gel-combustion routes

María Celeste Gardey Merino[a,b,*], Gustavo E. Lascalea[a], Laura M. Sánchez[c], Patricia G. Vázquez[d], Edgardo D. Cabanillas[e], Diego G. Lamas[c]

[a] Laboratorio de Investigaciones y Servicios Ambientales Mendoza (LISAMEN) – CCT – CONICET, Avda. Ruiz Leal s/n, Parque Gral. San Martín, (M5502IRA) Ciudad de Mendoza, Prov. de Mendoza, Argentina
[b] Grupo CLIOPE, Universidad Tecnológica Nacional – Facultad Regional Mendoza, Rodríguez 273, (M5502AJE) Ciudad de Mendoza, Prov. de Mendoza, Argentina
[c] CINSO (Centro de Investigaciones en Sólidos), CITEFA – CONICET, J.B. de La Salle 4397, (B1603ALO) Villa Martelli, Prov. de Buenos Aires, Argentina
[d] Centro de Investigación y Desarrollo en Ciencias Aplicadas "Dr. Jorge J. Ronco" (CINDECA), CONICET, Universidad Nacional de La Plata, Calle 47 nro. 257, (B1900AJK) La Plata, Prov. de Buenos Aires, Argentina
[e] CONICET and Centro Atómico Constituyentes, Comisión Nacional de Energía Atómica, Gral. Paz 1499, (1650) San Martín, Prov. de Buenos Aires, Argentina

ARTICLE INFO

Article history:
Received 12 August 2009
Accepted 6 October 2009
Available online 7 November 2009

Keywords:
Nanostructured materials
Oxide materials
X-ray diffraction

ABSTRACT

In this work, two new gel-combustion routes for the synthesis of Al_2O_3 nanopowders with aspartic acid as fuel are presented. The first route is a conventional stoichiometric process, while the second one is a non-stoichiometric, pH-controlled process. These routes were compared with similar synthesis procedures using glycine as fuel, which are well-known in the literature. The samples were calcined in air at different temperatures, in a range of 600–1200 °C. They were characterized by X-ray diffraction, scanning electron microscopy, transmission electron microscopy and BET specific surface area. Different phases were obtained depending on the calcination temperature: amorphous, γ (metastable) or α (stable). The amorphous-to-γ transition was found for calcination temperatures in the range of 700–900 °C, while the γ-to-α one was observed for calcination temperatures of 1100–1200 °C. The retention of the metastable γ phase is probably due to a crystallite size effect. It transforms to the α phase after the crystallite size increases over a critical size during the calcination process at 1200 °C. The highest BET specific surface areas were obtained for both nitrate–aspartic acid routes proposed in this work, reaching values of about 50 m^2/g.

1. Introduction

In recent years, increasing attention has been focused on the development of nanocrystalline alumina powders. γ-Al_2O_3 is an extremely important nanosized material considering its applications as a catalyst and catalyst support in the automotive and petroleum industries, in structural composites for spacecraft, miniature power supplies and abrasive and thermal wear coating. Ultrafine α-Al_2O_3 powder has considerable potential for a wide range of applications including high strength materials, electronic ceramics and catalysts.

Several wet-chemical routes have been proposed for the synthesis of nanocrystalline oxides. Particularly, gel-combustion processes proved to be useful for the synthesis of nanomaterials with high specific surface areas and excellent compositional homogeneity by simple and low-cost procedures [1–8]. These methods are based on the gelling and subsequent combustion of an aqueous solution containing salts of the desired metals (nitrates are usually preferred) and an organic fuel, such as glycine, citric acid, etc. The combustion process is due to an exothermic, redox reaction between nitrate ions and the fuel. The large volume of gases released during the reaction promotes a rapid disintegration of the precursor gel, yielding the desired nanocrystalline material. The characteristics of the powder, such as crystallite size, specific surface area, nature (hard or soft) of agglomeration, etc., are primarily governed by enthalpy and/or flame temperature generated during the combustion stage, which is dependent on the nature of the fuel and the fuel-to-oxidant ratio. This ratio is usually chosen close to that corresponding to a stoichiometric reaction, since the combustion process is faster under this condition. However, in previous works, we have demonstrated that pH-controlled gel-combustion processes with excess of nitrates render compositionally homogeneous, nanocrystalline powders with high specific surface areas [3–5]. Unfortunately, these routes have not been extensively explored yet.

In the present work, we investigated novel gel-combustion routes for the synthesis of Al_2O_3 nanopowders using aspartic acid as fuel by both stoichiometric and pH-controlled gel-combustion

* Corresponding author. Tel.: +54 0261 5243000; fax: +54 0261 5244531.
E-mail address: mcgardey@frm.utn.edu.ar (M.C. Gardey Merino).

0925-8388/$ – see front matter © 2009 Elsevier B.V. All rights reserved.
doi:10.1016/j.jallcom.2009.10.042

Table 1
Identified phases and average crystallite sizes of Al_2O_3 powders synthesized by the different gel-combustion routes studied in this work and calcined at different temperatures. Numbers in parentheses indicate the error in the last significant digit.

Sample		Present phase	Average crystallite size (nm)
Gel-combustion route	Calcination temperature (°C)		
Stoichiometric nitrate–aspartic acid	600	Amorphous	–
Stoichiometric nitrate–aspartic acid	900	γ	4.7 (2)
Stoichiometric nitrate–aspartic acid	1200	α	85 (5)
Non-stoichiometric nitrate–aspartic acid	600	Amorphous	–
Non-stoichiometric nitrate–aspartic acid	900	γ	8.5 (4)
Non-stoichiometric nitrate–aspartic acid	1200	α	$1.2\,(1)\times10^2$
Stoichiometric nitrate–glycine	600	Amorphous	–
Stoichiometric nitrate–glycine	800	γ	4.8 (2)
Stoichiometric nitrate–glycine	1200	α	45 (3)
Non-stoichiometric nitrate–glycine	600	Amorphous	–
Non-stoichiometric nitrate–glycine	800	γ	6.9 (3)
Non-stoichiometric nitrate–glycine	1200	α	$1.4\,(2)\times10^2$

routes. The use of aspartic acid as fuel has been recently proposed for the synthesis of other oxides by the stoichiometric gel-combustion process [8–10], but to our knowledge it has not been investigated for the synthesis of nanocrystalline Al_2O_3. This fuel is interesting due to its complex properties since it is a dicarboxylic amino acid. Besides, its enthalpy of combustion is higher than that of glycine [11]. We have studied different calcination temperatures, in the range of 600–1200 °C, in order to evaluate the influence of the crystallite size on the crystal structure. For the purpose of comparison, powders synthesized by similar gel-combustion processes using glycine as fuel were also analyzed.

2. Experimental procedure

2.1. Synthesis of Al_2O_3 nanopowders

Both gel-combustion routes studied in this paper using aspartic acid as organic fuel are described below. They were compared with similar processes using glycine as fuel. All the chemical routes were performed using reagents of analytical grade. The final calcination temperatures were in the range of 600–1200 °C.

2.1.1. Stoichiometric nitrate–aspartic acid route

7.5 g of $Al(NO_3)_3{\cdot}9H_2O$ (Merck) and 2.66 g of aspartic acid (Anedra) were dissolved in distilled water to obtain a homogeneous solution, with a total volume of 400 ml (pH 3). The aspartic acid/metal molar ratio was calculated on the basis of a stoichiometric combustion reaction:

$$2Al(NO_3)_3{\cdot}9H_2O + 2NH_2CH_2CH(COOH)_2 \rightarrow Al_2O_3 + 4N_2 + 8CO_2 + 25H_2O$$

This precursor solution was concentrated on a hot plate at 250 °C until a viscous gel was obtained. Soon after, it ignited and the combustion process proceeded softly, without flame.

This stoichiometric nitrate–aspartic acid route was compared with the conventional nitrate–glycine route (usually called "glycine–nitrate process", GNP [1,2]). The same procedure was used, starting from the same mass of $Al(NO_3)_3{\cdot}9H_2O$, but in this case the stoichiometric reaction requires a glycine/Al molar ratio of 5/3.

2.1.2. Non-stoichiometric pH-controlled nitrate–aspartic acid route

A first solution was prepared from 7.5 g of $Al(NO_3)_3{\cdot}9H_2O$ (Merck), 50 ml of distilled water and 50 ml of HNO_3 (concentrated, Merck). A second solution was prepared by dissolving 7.99 g of aspartic acid (Anedra) in 100 ml of distilled water and both solutions were mixed, thus resulting an aspartic acid/Al molar ratio of 3. This ratio was chosen based on the "oxidative valence criterion" [12], taking into account previous studies of similar processes, the optimum ratio for the pH-controlled nitrate–glycine route to synthesize ZrO_2–CeO_2 solid solutions was found to be 5 [4,5]. Then, NH_4OH (diluted, Merck) was added to obtain 300 ml of a precursor solution with pH 2. The solution pH was not further controlled after this stage. This solution was then concentrated on a hot plate at 250 °C until it turned into a viscous gel, which finally burned due to a vigorous exothermic reaction with a flaming stage of about 1 min.

This non-stoichiometric nitrate–aspartic acid route was compared with a similar pH-controlled nitrate–glycine process. The same procedure was used, but in this case the glycine/Al ratio was chosen as 5, the optimum ratio found in previous works for other oxides [4,5].

2.2. Characterization of Al_2O_3 nanopowders

The phases present in the as-synthesized Al_2O_3 nanopowders (obtained after calcination) were identified by X-ray diffraction (XRD) using a Philips PW 3710 diffractometer operated with Cu-K_α radiation. Our data were compared with those

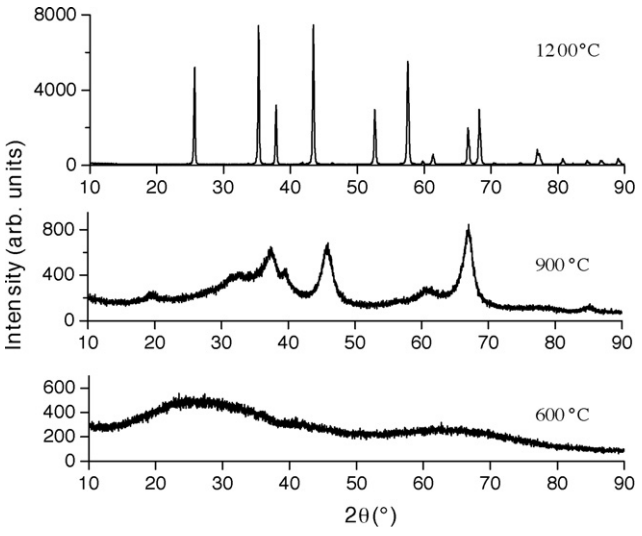

Fig. 1. XRD patterns of Al_2O_3 nanopowders synthesized by stoichiometric nitrate–aspartic acid gel-combustion routes calcined at different temperatures.

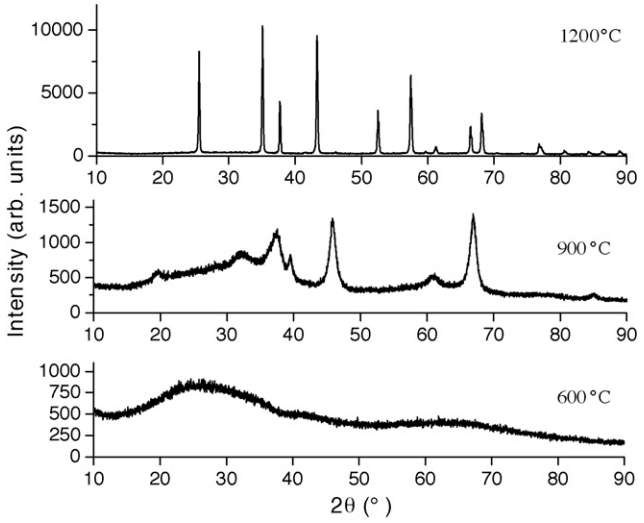

Fig. 2. XRD patterns of Al_2O_3 nanopowders synthesized by non-stoichiometric pH-controlled nitrate–aspartic acid gel-combustion routes calcined at different temperatures.

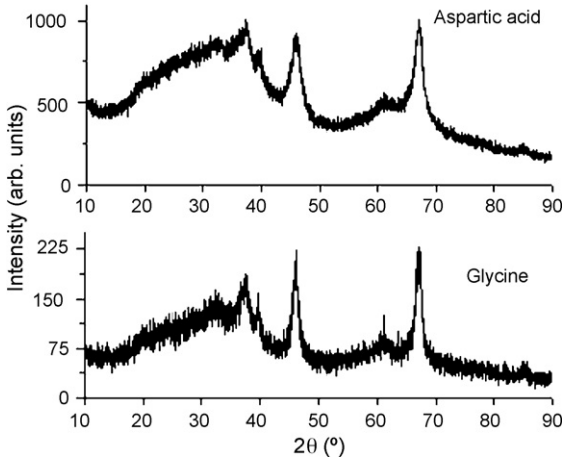

Fig. 3. Comparison between XRD patterns of Al_2O_3 nanopowders synthesized by stoichiometric nitrate–aspartic acid and nitrate–glycine routes calcined at 800 °C.

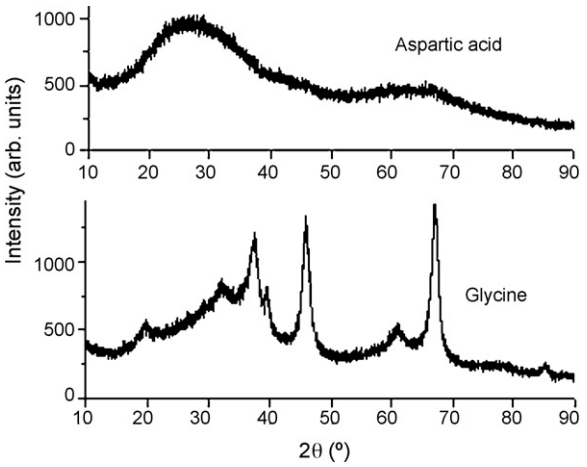

Fig. 4. Comparison between XRD patterns of Al_2O_3 nanopowders synthesized by non-stoichiometric pH-controlled nitrate–aspartic acid and nitrate–glycine routes calcined at 800 °C.

reported in the inorganic crystal structure database (ICSD). The crystallite size was determined from the broadening of Bragg peaks using the Scherrer equation [13]:

$$D = \frac{0.9\lambda}{\beta \cos\theta} \quad (1)$$

where D is the crystallite size, λ is the wavelength of the radiation (1.5418 Å for Cu-K_α radiation), β is the corrected peak width at half-maximum intensity and θ is the peak position. Since the line shape was approximately Lorentzian for all the samples, the value of b was corrected using the formula $\beta = \beta_m - \beta_i$, where β_m is the measured peak width and β_i is the instrumental broadening, which was determined using an α-Al_2O_3 powder with a mean particle diameter of 25 μm.

The morphology of the powders was analyzed by scanning electron microscopy (SEM, Philips 515 microscope) and transmission electron microscopy (TEM, Philips EM 300 microscope). The operation voltage was between 10 and 20 kV for SEM study and 100 kV for TEM one. In both cases, the preparation of samples was performed following conventional procedures.

The specific surface areas of the powders were measured by the multipoint Brunauer–Emmett–Teller (BET) adsorption technique using a Micromeritics Accusorb 2100E equipment.

3. Results and discussion

Al_2O_3 nanopowders synthesized by the new gel-combustion routes proposed in this work using aspartic acid as fuel exhibited similar characteristics to those obtained by the conventional nitrate–glycine routes.

Table 1 summarizes the main results obtained by XRD for all the gel-combustion routes investigated in this work. XRD data showed that all powders exhibited the amorphous phase after calcination at 600 °C. The phase transformations, amorphous-to-γ and γ-to-α, proceeded with increasing calcination temperature, as shown in Figs. 1 and 2. The metastable γ phase was fully retained after calcination at temperatures in the range of 800–900 °C, depending on the synthesis route. In Figs. 3 and 4, it can be noticed that nanopowders synthesized by both glycine routes fully transformed to the γ phase after calcination at 800 °C, while the sample synthesized by stoichiometric nitrate–aspartic acid route exhibited a mixture of γ and amorphous phases and that synthesized by non-stoichiometric pH-controlled nitrate–aspartic acid route was amorphous. The average crystallite size of nanopowders exhibiting the γ phase was in the range of 5–9 nm. The smallest crystallite sizes were obtained for samples synthesized by stoichiometric routes, being very similar for both of them.

The γ-to-α transition occurs for calcination temperatures of 1100–1200 °C, due to crystallite growth. The average crystallite size of the samples calcined at 1200 °C varied in the range of 45–140 nm. The smallest average crystallite size (45 nm) was obtained by the stoichiometric nitrate–glycine route.

SEM observations showed that all the samples exhibited a high degree of agglomeration, with large "flake-like" aggregates, as observed in Figs. 5 and 6. Amorphous samples did not exhibit any substructure, while small particles were detected in both γ and α samples.

TEM observations confirmed that the γ and α samples were composed of aggregates of small particles. Bright-field TEM micrographs (Fig. 7) showed particles with typical sizes close to the crystallite size determined from XRD data, that also agrees with the sizes determined by dark-field TEM observations. In the case of the nanopowders exhibiting the amorphous phase, we found a morphology similar to that of γ samples with very small particles, but electron diffraction patterns confirmed their amorphous crystal structure.

BET specific surface areas resulted in agreement with the above SEM and TEM observations. For example, Table 2 summarizes the results obtained by both nitrate–aspartic acid gel-combustion routes, after calcination at different temperatures. It can be observed that the highest values were found for samples exhibiting the γ phase, while amorphous or α samples exhibited much lower values. Table 3 presents the BET specific surface areas obtained for γ samples synthesized for all the routes studied in this work, calcined at 900 °C. The highest values were obtained for both nitrate–aspartic acid routes proposed in this work, reaching values of about 50 m^2/g.

Table 2
BET specific surface areas of Al_2O_3 samples synthesized by both nitrate–aspartic acid gel-combustion routes proposed in this work, calcined at different temperatures.

Sample		BET specific surface area (m^2/g)
Gel-combustion route	Calcination temperature (°C)	
Stoichiometric nitrate–aspartic acid	600	22.8
Stoichiometric nitrate–aspartic acid	900	52.3
Stoichiometric nitrate–aspartic acid	1200	6.0
Non-stoichiometric nitrate–aspartic acid	600	16.4
Non-stoichiometric nitrate–aspartic acid	900	51.9
Non-stoichiometric nitrate–aspartic acid	1200	12.7

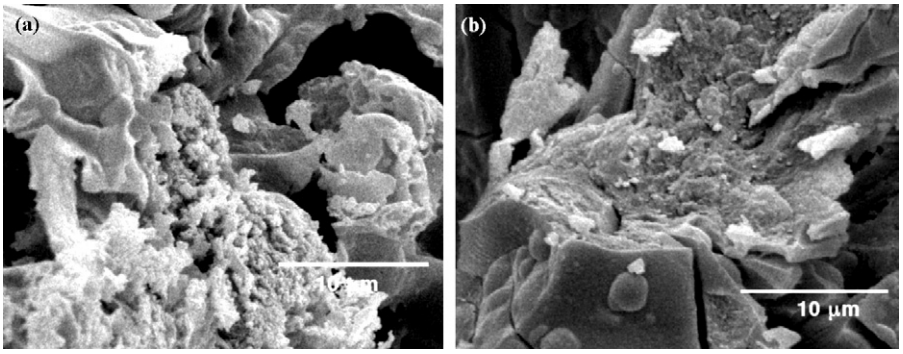

Fig. 5. SEM micrographs of Al_2O_3 nanopowders exhibiting the metastable γ phase. (a) Non-stoichiometric nitrate–aspartic acid route calcined at 900 °C. (b) Stoichiometric nitrate–aspartic acid route calcined at 850 °C.

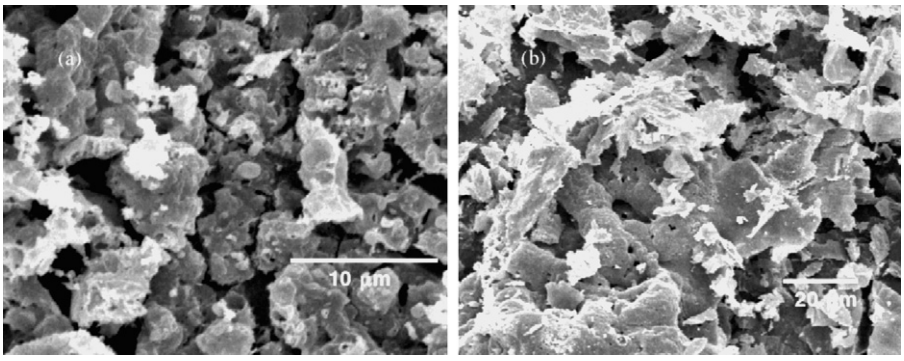

Fig. 6. SEM micrographs of Al_2O_3 nanopowders exhibiting the α phase. (a) Non-stoichiometric nitrate–glycine route calcined at 1200 °C. (b) Non-stoichiometric nitrate–aspartic acid route calcined at 1200 °C.

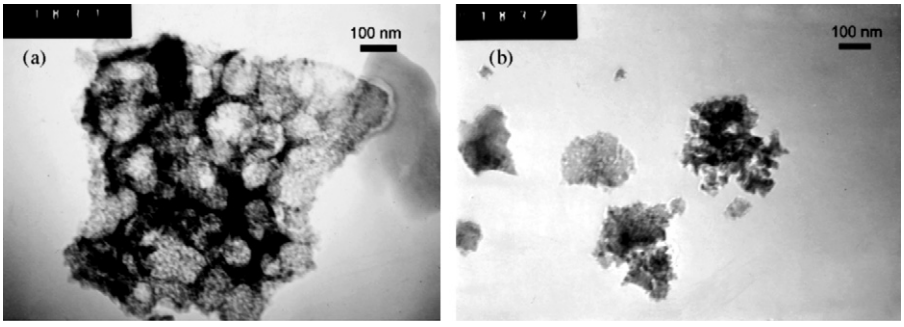

Fig. 7. TEM micrographs showing the typical morphology of Al_2O_3 nanopowders exhibiting the metastable γ phase. (a) Stoichiometric nitrate–aspartic acid route calcined at 850 °C. (b) Stoichiometric nitrate–glycine acid route calcined at 800 °C.

Table 3
BET specific surface areas of Al_2O_3 samples exhibiting the γ phase, synthesized by all gel-combustion routes studied in this work and calcined at 900 °C.

Gel-combustion route	BET specific surface area (m^2/g)
Stoichiometric nitrate–aspartic acid	52.3
Non-stoichiometric nitrate–aspartic acid	51.9
Stoichiometric nitrate–glycine	13.7
Non-stoichiometric nitrate–glycine	36.5

Taking into account the interesting results found in this work, a systematic study of the influence of the synthesis parameters on powder morphology will be performed in the near future.

4. Conclusions

Both nitrate–aspartic acid gel-combustion processes proposed in this work allow the synthesis of Al_2O_3 nanopowders with similar characteristics to those synthesized using glycine as fuel. All powders exhibited the amorphous phase after calcination at 600 °C and transform to γ and α phases with increasing calcination temperature. The critical calcination temperature for the amorphous-to-γ phase transition depends on the synthesis route. The γ-to-α transition occurs for calcination temperatures of 1100–1200 °C, due to crystallite growth. γ samples exhibited the highest BET specific surface areas, reaching values of about 50 m^2/g for both nitrate–aspartic acid routes.

Acknowledgements

The authors thank Agencia Nacional de Promoción Científica y Tecnológica (Argentina, PICT 38309) for financial support, CNEA for the use of their electron microscope facilities and Lic. Mariana Rosenbusch (CONICET) for her assistance during SEM observations. M.C. Gardey Merino thanks National Technological University for the Doctoral Scholarship Res. No. 175/2007 and the authorities of

LISAMEN – CCT – CONICET, Mendoza, for allowing her to perform a research stay (March–October 2008) for experimental work in synthesis of nanostructured materials.

References

[1] L.A. Chick, L.R. Pederson, G.D. Maupin, J.L. Bates, L.E. Thomas, G.J. Exarthos, Mater. Lett. 10 (1990) 6–12.
[2] L.R. Pederson, G.D. Maupin, W.J. Weber, D.J. McReady, R.W. Stephens, Mater. Lett. 10 (1991) 437–443.
[3] R.E. Juárez, D.G. Lamas, G.E. Lascalea, N.E. Walsöe de Reca, J. Eur. Ceram. Soc. 20 (2000) 133–138.
[4] D.G. Lamas, G.E. Lascalea, R.E. Juárez, E. Djurado, L. Pérez, N.E. Walsöe de Reca, J. Mater. Chem. 13 (2003) 904–910.
[5] G.E. Lascalea, D.G. Lamas, L. Pérez, E.D. Cabanillas, N.E. Walsöe de Reca, Mater. Lett. 58 (2004) 2456–2460.
[6] K.C. Patil, S.T. Aruna, T. Mimani, Curr. Opin. Sol. State Mater. Sci. 6 (2002) 507–512.
[7] S.T. Aruna, A.S. Mukasyan, Curr. Opin. Sol. State Mater. Sci. 12 (2008) 44–50.
[8] S.T. Mukherjee, V. Bedekar, A. Patra, P.U. Sastry, A.K. Tyagi, J. Alloys Compd. 466 (2008) 493–497.
[9] A. Subramania, N. Angayarkanni, N. Niruba, T. Vasudevan, Nanotechnology 18 (2007), art.065603.
[10] T. Saradha, S. Muzhumathi, A. Subramania, J. Solid State Electrochem. 12 (2008) 143–148.
[11] X.W. Yang, J.R. Liu, S.L. Gao, Y.D. Hou, Q.Z. Shi, Thermochim. Acta 329 (1999) 109–115.
[12] S.R. Jain, K.C. Adiga, V.R. Pai Verneker, Combust. Flame 40 (1981) 71–79.
[13] H. Klug, L. Alexander, X-ray Diffraction Procedures for Polycrystalline and Amorphous Materials, second ed., John Wiley and Sons, New York, 1974.